Available online at www.sciencedirect.com
ScienceDirect
Energy Procedia 8 (2011) 487–492
Energy Procedia

SiliconPV: 17-20 April 2011, Freiburg, Germany

Influence of the Front Surface Passivation Quality on Large Area n-Type Silicon Solar Cells with Al-Alloyed Rear Emitter

F. Book[a,]*, T. Wiedenmann[a], G. Schubert[b], H. Plagwitz[b], G. Hahn[a]

[a]*University of Konstanz, Department of Physics, P.O. Box X916, 78457 Konstanz, Germany*
[b]*Sunways AG, Macairestraße 3-5,78467 Konstanz, Germany*

Abstract

Efficiencies of large area n-type silicon solar cells with a screen printed rear side aluminum-alloyed emitter are mainly limited by their front surface recombination velocity. The front surface therefore has to be passivated by an effective passivation layer combined with a front surface field (FSF).
In this work we investigate the influence of the front surface passivation quality and the base resistivity for a selective FSF n-type solar cell. The potential of this solar cell concept is assessed by PC1D simulations and QSSPC measurements. Furthermore we present solar cell results of all screen printed large area n-type Cz-Si solar cells with an aluminum rear emitter and a selective etch-back FSF passivated by a PECVD-SiN_x or a SiO_2/SiN_x stack. The applied processing sequence is based on industrially available processing equipment and results in an independently confirmed cell efficiency of 19.4 % on a 6" solar cell.

Selection and/or peer-review under responsibility of SiliconPV 2011

n-type; Al emitter; selective

1. Introduction

The standard processing sequence for industrial screen printed p-type Cz silicon solar cells is well optimized, but it suffers from a rather low bulk lifetime which is caused by the boron and oxygen related light induced degradation [1]. This limitation can be overcome by using n-type silicon, which does not contain any boron and is more tolerant for metal impurities [2]. Applying the standard processing

* Corresponding author. Tel.: +49-7531-882074; fax: +49-7531-883895.
E-mail address: felix.book@uni-konstanz.de

1876–6102 © 2011 Published by Elsevier Ltd. Selection and/or peer-review under responsibility of SiliconPV 2011.
Open access under CC BY-NC-ND license. doi:10.1016/j.egypro.2011.06.170

sequence to n-type silicon leads to a rear emitter solar cell with a phosphorous front surface field [3]. Since the electron-hole pairs are mainly generated close to the front surface of the solar cell, a high bulk lifetime and an effective front surface passivation are crucial for achieving high efficiencies with this solar cell type. Since its first publication in 2001 [3], large improvements have been achieved by several groups [4–10]. Possible approaches to achieve the required surface passivation quality are a SiO_2/SiN_x stack, a high ohmic FSF combined with advanced front contact technology [7] or a selective FSF [8–10].

In this work, we combine the well known SiO_2/SiN_x stack with a selectively etched back FSF. Due to the very low surface phosphorous concentration of the etch-back FSF, an extremely low front surface recombination velocity (SRV) can be achieved by this passivation system. The potential of this solar cell concept is assessed by PC1D simulations [11] and quasi-steady state photoconductance (QSSPC) measurements, furthermore we present solar cell results for a plasma-enhanced chemical vapor deposition (PECVD)-SiN_x and a SiO_2/SiN_x stack as passivation layers for an etch-back FSF.

2. PC1D simulations

The major difference arising from applying the standard solar cell process to n- instead of p-type silicon is the location of the p/n-junction at the rear side of the cell. This leads to a different influence of the passivation quality and base resistivity on the solar cell IV characteristics (compare e.g. [12]). These effects are illustrated by PC1D simulations using the following parameters if not specified differently:

Thickness:	175 µm
Net τ_{lli}:	20 ms
Front SRV:	$5{\cdot}10^4$ cm/s
Rear SRV:	$1{\cdot}10^7$ cm/s
Doping profiles:	from ECV measurement. FSF: 30 Ω/sq etched back to 100 Ω/sq
Front reflectance:	from reflectance measurement including metallization

2.1. Front SRV

The Front SRV affects the collection probability of minority charge carriers by the rear emitter over the whole solar cell depth, since even for long wavelengths a considerably large part of the electron-hole pairs is generated close to the front surface. The effect on the internal quantum efficiency (IQE) and the IV data is shown in Fig. 1.

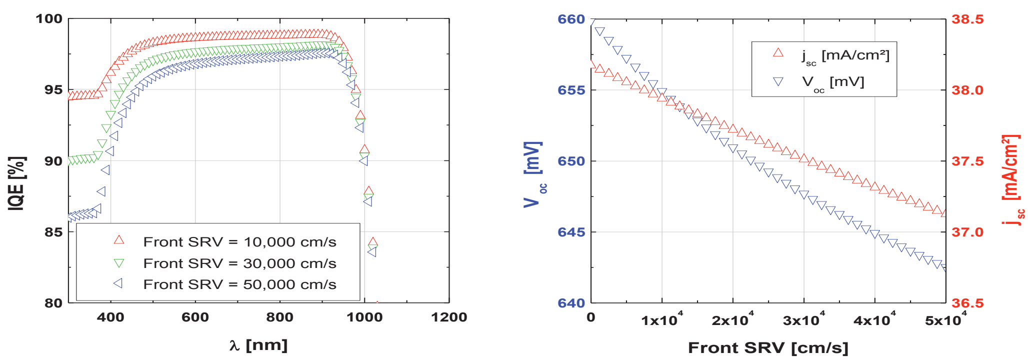

Fig. 1. (a) Influence of the Front SRV on the IQE (b) j_{sc} and V_{oc} vs. Front SRV

2.2. Base doping

The influence of the base resistivity on j_{sc} and V_{oc} depends on the front surface passivation quality (see Fig. 2a). A low base resistivity reduces the difference in doping concentration between the base and the front surface leading to a lower injection level in the base and therefore a reduced V_{oc} for a low ohmic substrate (see Fig. 2b). At j_{sc} the base injection level is similar for the high and low ohmic substrate, but the less effective FSF results in a higher hole density at the surface for the low ohmic substrate (compare [13]). If the surface is not well passivated, this leads to higher surface recombination losses for a low base resistivity. It also means that the influence of the resistivity can be reduced by a high passivation quality.

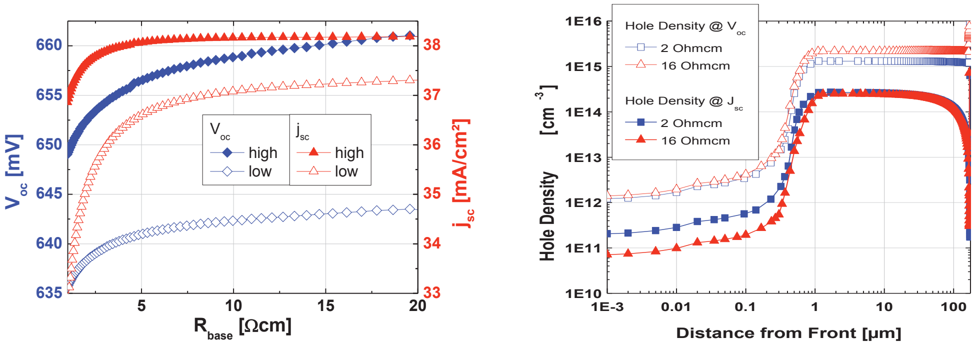

Fig. 2. (a) j_{sc} and V_{oc} vs. base resistivity for a high (SRV = $5\cdot10^3$ cm/s, $N_S = 4.5\cdot10^{19}$ cm^{-3}) and low (SRV = $5\cdot10^4$ cm/s, $N_S = 2\cdot10^{20}$ cm^{-3}) surface passivation quality (b) Hole density at j_{sc} and V_{oc} for 2 and 16 Ωcm n-type silicon with a 100 Ω/sq FSF

2.3. Effective sheet resistance

On a rear junction n-type solar cell, the lateral conductivity between the front grid lines is provided not only by the FSF but also by the base, since it has the same polarity. As a first approximation the FSF and the base can be regarded as parallel connected resistances (see e.g. [9]). When calculating the contribution from the base, the injection level has to be accounted for, since at the maximum power point (MPP) and at V_{oc} the base is not under low level injection conditions. This leads to an injection level dependent effective sheet resistance (see Fig. 3).

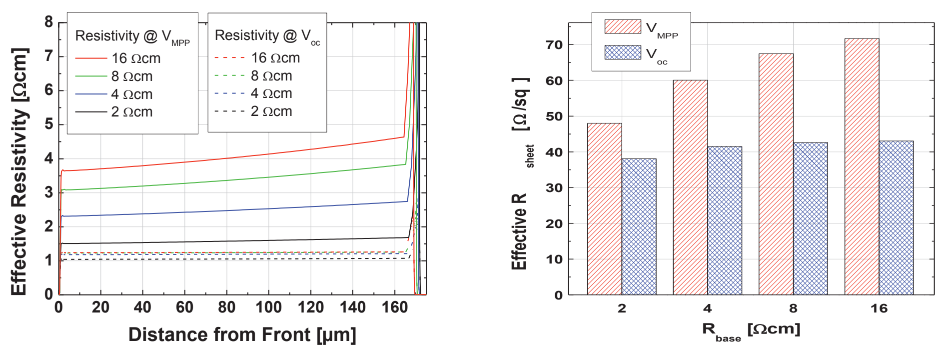

Fig. 3. (a) Resistivity under 1 sun illumination for different base doping concentrations at V_{MPP} and V_{oc}. (b) Effective sheet resistance under illumination (integrated from the front surface to the p/n-junction) for different base doping concentrations combined with a 100 Ω/sq etch-back FSF at V_{MPP} and V_{oc}

3. Experimental results

We investigate the potential of two different passivation layers as a front side passivation for rear junction n-type solar cells with a selectively etched back FSF:

- Standard PECVD-SiN_x (n = 2.0)
- 10 nm dry thermal oxide + standard PECVD-SiN_x (n = 2.0)

3.1. Passivation Quality

The passivation quality of the two layers is characterized by QSSPC measurements under high level injection conditions on symmetrical 200 Ωcm p-type FZ wafers with a $POCl_3$ emitter etched back from 30 Ω/sq to various sheet resistances. On all samples, the sheet resistance was measured by four point probing between the etch-back and the deposition of the passivation layer.

Fig. 4a shows the results for chemically polished and random pyramid textured wafers. With the SiO_2/SiN_x stack layer extremely low saturation currents of < 20 fA/cm² were achieved on both surfaces. The thermal oxidation also has a drive-in effect on the doping profile (see Fig. 4b) which leads to a reduced surface phosphorous concentration especially for an etch-back to < 100 Ω/sq where the kink of the profile is still present. This also explains the steeper decay of j_{0E} with R_{sheet} for the oxidized samples with R_{sheet} < 100 Ω/sq.

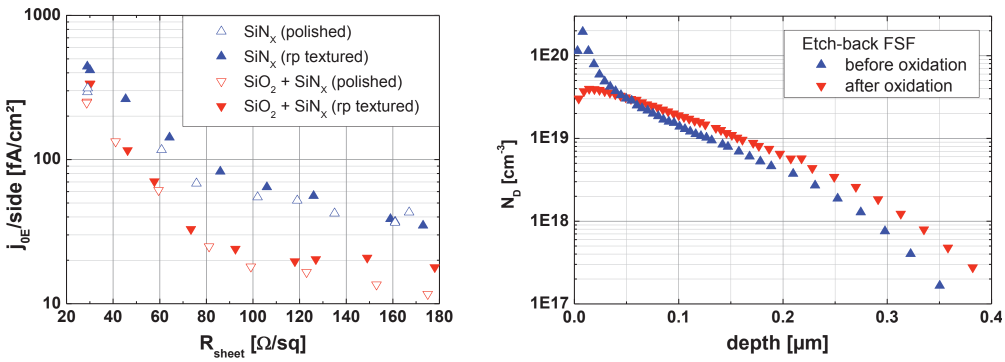

Fig. 4. (a) Saturation current density vs. sheet resistance of random pyramid textured and chemically polished samples with an FSF etched back from 30 Ω/sq to various sheet resistances and passivated by a PECVD-SiN_x layer or a thermal SiO_2/SiN_x stack. The j_{0E} values are evaluated at a minority carrier density of $1 \cdot 10^{16}$ cm^{-3} assuming an intrinsic carrier density n_i of $8.6 \cdot 10^9$ cm^{-3}
(b) ECV doping profile of an etch-back FSF before and after the thermal oxidation

3.2. Solar cell results

According to the processing sequence described in [8], all screen printed solar cells with a selective etch-back FSF and an unpassivated full area Al alloyed emitter were processed from 6” Cz n-type wafers with a base resistivity of 6 Ωcm (material A, thickness after texture: 220 µm) and 11 Ωcm (material B, thickness after texture: 180 µm). The FSF was passivated by a PECVD-SiN_x layer and a SiO_2/SiN_x stack. For the latter, the HCl/HF clean before the deposition of the passivation layer was replaced by a RCA clean. The base resistivity was measured by an electrochemical capacitance voltage (ECV) profiler (WEP CVP21) after all high temperature process steps.

On all cells the edges which are not covered by Al paste at the rear (approx. 1 mm) were cut off by an automatic dicing saw. Since on these edges no emitter is formed, they do not contribute to I_{sc} and therefore reduce j_{sc}. Removing them leads to an average increase in cell efficiency of 0.3 $\%_{abs}$. The average IV results obtained after removing the edges are presented in table 1.

Table 1. Average IV data (4–6 cells/group) from 6 Ωcm and 11 Ωcm 6” n-type Cz silicon (100 % Al emitter coverage). The lower j_{sc} values of the 6 Ωcm cells are due to an increased finger width (120–160 µm) caused by a worn out screen

Base Material	FSF Passivation	V_{oc} [mV]	j_{sc} [mA/cm^2]	FF [%]	η [%]
A (6 Ωcm)	SiN_x	642	36.5	79.7	18.7
	$SiO_2 + SiN_x$	649	37.1	79.9	19.2
B (11 Ωcm)	SiN_x	641	37.1	79.5	18.9
	$SiO_2 + SiN_x$	649	37.5	79.8	19.4
Best cell (confirmed by ISE CalLab)		647	37.6	79.8	19.4

On both substrates very high V_{oc} values up to 650 mV were measured. The lower j_{sc} values achieved on the cells from material A are caused by an increased finger width (120–160 µm) due to a worn out screen. The associated reflection loss was calculated from the reflexion data to 0.5 mA/cm² compared to material B on which a new screen was used.

The high fill factors are mainly caused by a very low j_{02} of 1.2–1.6·10^{-8} A/cm². Compared to a typical value of 2·10^{-8} A/cm² for a p-type solar cell, this leads to a gain in fill factor of approx. 0.5 %.

With additional SiO_2 layer, an average increase of 0.58 $\%_{abs}$ for material A and 0.54 $\%_{abs}$ for material B was achieved. The influence of the improved surface passivation on the IQE is shown in Fig. 5.

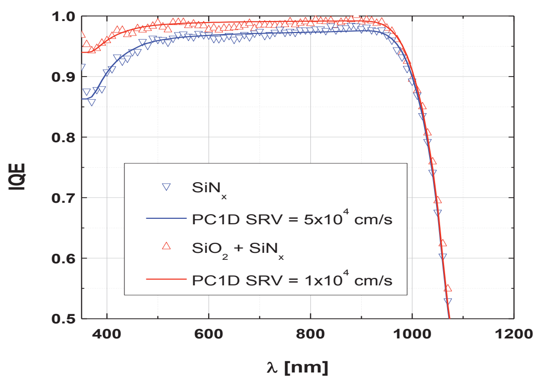

Fig. 5. IQE of a rear junction n-type solar cell with a FSF passivation of PECVD-SiN_x or a SiO_2/SiN_x stack. The PC1D simulation was performed using the doping profiles before and after the thermal oxidation (see Fig. 4b)

4. Conclusion

For rear emitter n-type solar cells, a good front surface passivation quality is the key to achieve high efficiencies. Besides increasing j_{sc} and V_{oc}, an enhanced surface passivation reduces the influence of the base resistivity. A wider range of resistivity can therefore be used for this cell type.

We have shown that under illumination the effective sheet resistance from the FSF and the base is significantly reduced by the photoconductivity, since the base is not under low injection conditions. On low ohmic base material the FSF is therefore not necessary to maintain a good lateral conductivity. For these substrates, an etch-back to very low surface phosphorous concentrations could therefore be preferable to achieve an even better surface passivation.

The excellent passivation quality of the etch-back FSF combined with PECVD-SiN_x or a SiO_2/SiN_x stack was demonstrated by QSSPC measurements. Furthermore we have presented solar cell results for all screen printed 6” n-type solar cells with an unpassivated full area Al-alloyed emitter. A highest independently confirmed cell efficiency of 19.4 % was achieved. Compared to a standard PECVD-SiN_x passivation, the SiO_2/SiN_x stack has led to an increase in cell efficiency of approx. 0.5 $\%_{abs}$.

Acknowledgements

The financial support from the German Federal Ministry of Education and Research under contract No. 03SSF0335I and the BMU project 0325079 is gratefully acknowledged in particular for the processing and characterization equipment. The authors furthermore would like to thank A. Herguth, S. Graf, D. Kiliani, B. Rettenmaier, S. Ohl, L. Mahlstaedt, J. Ruck, F. Mutter and C. Gründler for the characterization and processing support. The content of this publication is the responsibility of the authors.

References

[1] Glunz SW, Rein S, Lee JY, Warta W. Minority Carrier Lifetime Degradation in Boron-Doped Czochralski Silicon. *J Appl Phys* 2001;**90**:2397-404.

[2] Macdonald D, Geerligs LJ. Recombination Activity of Interstitial Iron and Other Transition Metal Point Defects in p- and n-Type Crystalline Silicon. *Appl Phys Lett* 2004;**85**:4061-3.

[3] Meier DL, Davis HP, Garcia RA, Salami J, Rohatgi A, Ebong A et al. Aluminum Alloy Back p-n Junction Dendritic Web Silicon Solar Cell. *Solar Energy Materials and Solar Cells* 2001;**65**:621-7.

[4] Buck T, Libal J, Eisert S, Kopecek R, Peter K, Fath P et al. Low Cost p+nn+-Type Back Junction Solar Cells by Screen Pinting Technique on Cz and mc-Si Material. *Proc. 19th EU PVSEC,* Paris 2004, p. 1255-8

[5] Mihailetchi VD, Sainova DS, Geerligs LJ, Weeber AW. 17.4% Efficiency Solar Cells on Large-Area and Thin n-Type Silicon with Screen-Printed Aluminum-Alloyed Rear Emitter. *Proc. 22nd EU PVSEC*, Milan 2007, p. 837-40

[6] Kopecek R, Halm A, Popescu L, Peter K, Vázquez MA, Fukushima N. Aluminium Rear Emitter Large Area n-Type Cz-Si Solar Cells for Industrial Application. *Proc. 25th EU PVSEC,* Valencia 2010, p. 2381-6

[7] Schmiga C, Rauer M, Rüdiger M, Meyer K, Lossen J et al. Aluminium-Doped p+ Silicon for Rear Emitters and Back Surface Fields: Results and Potentials of Industrial n- and p-Type Solar Cells. *Proc. 25th EU PVSEC,* Valencia 2010, p. 1163-8

[8] Veschetti Y, Schultz-Kuchly T, Cabal R, Sanzone V, Heslinga D. High Efficiency Solar Cells by Optimization of Front Surface Passivation on n-Type Rear Al Alloyed Emitter Structure. *Proc. 25th EU PVSEC,* Valencia 2010, p. 2265-7

[9] Meyer K, Schmiga C, Jesswein R, Dupke M, Lossen J, Krokoszinski HJ et al. All Screen-Printed Industrial n-Type Czochralski Silicon Solar Cells with Aluminium Rear Emitter and Selective FSF. *Proc. 35th IEEE PVSC*, Honolulu 2010, p. 3531-5

[10] Book F, Wiedenmann T, Dastgheib-Shirazi A, Raabe B, Hahn G. Large Area n-Type Silicon Solar Cells with Selective Front Surface Field and Screen Printed Aluminum-Alloyed Rear Emitter. *Proc. 25th EU PVSEC,* Valencia 2010, p. 1465-8

[11] Clugston DA, Basore PA. PC1D Version 5: 32-bit Solar Cell Modeling on Personal Computers, *Proc. 26th IEEE PVSC*, Anaheim, 1997, p. 207-10

[12] Ruediger M, Schmiga C, Rauer M, Hermle M, Glunz SW. Optimization of Industrial n-Type Silicon Solar Cells by Means of 2D Numerical Simulation. *Proc. 25th EU PVSEC,* Valencia 2010, p. 2280-6

[13] Hermle M, Granek F, Schultz O, Glunz SW. Analyzing The Effects of Front-Surface Fields on Back-junction Silicon Solar Cells Using the Charge-collection Probability and the Reciprocity Theorem. *J Appl Phys* 2008;**103**:054507.